Tellus (1987), *39A*, 397–407

Heating by organized convection as a source of polar low intensification

By HANS ØKLAND, *Institute of Geophysics, University of Oslo, P.O. Box 1022, Blindern, 0315 Oslo 3, Norway*

(Manuscript received 23 May; in final form 17 October 1986)

ABSTRACT

The paper discusses some observed characteristics which have not been taken into account in previous theoretical studies. For instance, a well-mixed convective boundary layer is a common feature of the synoptic situation when polar lows are observed. However, in the polar lows themselves, the convection seems to reach much higher levels. Also, many polar lows have a characteristic central domain with especially strong winds and large vorticity.

A simple linear CISK model is used to estimate the intensification caused by the convection. The model is based on constraints imposed by the assumption of a well-mixed convective layer. Elements of the cloud physics are used to explain observed characteristics of clouds and precipitation. Finally, it is shown that additional growth rate may be expected if CISK is present in an environment of large relative vorticity. An observed case is studied in the light of the general ideas set forth in this paper.

1. Introduction

In the weather service, polar lows have for a long time been associated with the instabilization of cold air masses over the relatively warm water of the Norwegian Sea. In fact, the connection with outbreaks of cold air masses has recently been verified in climatological studies (Businger, 1985; Ese et al., 1985). However, the reason for their generation is still obscure. Baroclinic instability, originally proposed by British meteorologists, has to some extent been verified by numerical simulations (Grønås et al., 1987), while Rasmussen (1979) and others have suggested that heating by cumulus convection may be the source of the vortices. Probably, both processes may contribute, although it is difficult to see how some of the really small-scale lows can be produced exclusively by baroclinic instability. On the other hand, heating by cumulus convection is hampered by the smallness of the water vapour mixing ratio. Also, it must be realized that the cumulus convection is part of a general air mass transformation in which sensible heat flux may be equally important in the arctic climate. These facts, and other connected circumstances, raise several complicated questions which we feel have not previously been taken seriously into account.

Usually, the cold air enters the Norwegian Sea from the ice-covered polar area. In the original stable air mass, a convective boundary layer forms. Its thickness at a certain location depends on several parameters, for instance the air-sea temperature difference along the trajectory. Here we shall specifically consider the circumstance that it is a function of the vertical temperature profile in the source area, which varies within wide limits. Computations based on equations formulated elsewhere (Økland, 1983) show that for a mean vertical temperature lapse rate of 0.005 K m^{-1}, the characteristic thickness may be in the range of 2000–3000 m in the southern part of the Norwegian Sea, in fair agreement with numerous observations. Nevertheless, convection has been observed to reach the height of 5000 m or more in some cases. Such a deep convection must be caused by a comparatively weak static stability of the ambient air and may not necessarily be present over an extended area. We shall consider this point more carefully later.

The convective boundary layer is well mixed, which means that conservative variables are nearly constant in the vertical direction. In fact, such layers are often modelled on this basis (Schubert et al., 1979). Conservative variables are potential temperature in the case of dry convection, and wet bulb potential temperature for moist convection. Consequently, the temperature profile conforms approximately with the dry adiabat below the lifting condensation level, and with the pseudo-adiabat above. Another conservative variable may be the water vapour mixing ratio, or, if condensation takes place, the mixing ratio of the total water substance, all three phases taken together (Lilly, 1968).

The fact that the convection takes place in a marginally unstable layer, is different from preferred regions for tropical cyclones where moist convection penetrates air which has a strong conditional instability (Ooyama, 1969). As we shall see, this has important aspects for a CISK-type process.

The characteristic time for adjustment towards an adiabatic lapse rate of a well-mixed layer is of the order 1 h (Lilly, 1968). Since this time is short in relation to the characteristic time for polar low development, we may assume that the convective boundary layer adjusts instantaneously to the adiabatic temperature profile. The physical mechanism for this adjustment is easily understood. For instance, excessive heating of an upper layer leads to stabilization beneath the layer. Accordingly, there must be an increased rate of heating of the air between the sea surface and the stable layer, thus eliminating the potential temperature inversion. We mention this point specifically since it shows that heating above the condensation level and none below is impossible under such conditions.

There is evidence indicating that polar lows tend to be associated with relatively deep convection. In fact, K. Wilhelmsen (personal communication) has found that in most cases with strong winds, the pseudo-adiabatic layer reaches at least up to 500 hPa. Several studies indicate a rapid increase in the depth of the convection during the approach of a polar low (see also Section 5 of the present paper).

Additional support for the above conclusion may be derived from satellite pictures. So-called comma clouds or cirrus shields seem to be present above nearly any polar low. Unfortunately, the height of these clouds has been determined only in a few cases. Those known to the author indicate heights in the range 400–600 hPa. In some cases, the clouds of a convective boundary layer may be distinguished below the cirrus as a stratocumulus cover. The cirrus clouds may, or may not, be connected to the convection. In the former case, there must somewhere be comparatively high cumulonimbus clouds from which anvil clouds may spread with the upper winds above the surrounding convective boundary layers of lesser height. On the other hand, no connection with the convection would presumably mean that the polar low is generated primarily at higher altitudes by processes not directly tied to the convection. The one possibility does not necessarily exclude the other, as we shall indicate at a later stage. However, since the former one agrees with the observation already mentioned, namely that a deep pseudo-adiabatic layer seems to be present in most polar lows, we shall pursue this alternative in the following.

Polar lows have been shown to give considerable precipitation (Rabbe, 1975, 1987). This indicates that the released latent heat may play a rôle in their development. The convective layer usually contains some wide-spread snow showers. A possible reason for the excessive precipitation may be the circumstance previously mentioned that the convective layer seems to be deeper in the low than in the surrounding atmosphere, meaning that the cloud tops are higher and colder. A larger part of the vapour contained in a rising bubble of air may then be condensed. Moreover, the growth of the falling ice crystals by accretion and aggregation must be more effective since the time spent in the cloud is longer. This growth, believed to be of paramount importance for the formation of precipitation is, in fact, an accelerating process (see, for instance, Wallace and Hobbs, 1977). Therefore, a modest increase in the depth of the clouds may produce a large increase in the intensity of the precipitation.

Seen from another point of view, precipitation appears to be a necessary requisite for CISK under the condition described. In the typical formulation, this mechanism for amplification consists in relating the convergence of vapour to the gross heating of the central part of the low, thus creating a secondary circulation and an associated increase in the primary circulation (see, for instance, Holton, 1979). Water vapour is supplied to the air by the surface fluxes, and tends to be evenly distributed through a vertical column in the convective layer. Condensation makes no difference if the total content of the water substance is considered. There may be horizontal gradients caused by spatial differences in the fluxes. If these differences can be disregarded, the mixing ratio will be approximately constant through the whole layer. Ekman layer convergence may lead to a net release of latent heat in the central part of the low. However, evaporation in the corresponding downdraft at greater radii (and higher pressure) causes cooling by the same amount. Additional heat (i.e., surface fluxes) is assumed to be stored as internal energy and turbulence. Then, according to the theorem of Sandström, a secondary circulation cannot be sustained since the heat sink is at higher pressure than the heat source (Eliassen and Kleinschmidt, 1957). On the other hand, precipitation in the central part reduces the content of water in the downdraft. This makes the cooling smaller than the heating, and the cited theorem does not apply.

In conclusion, we may say that significant heating by condensation seems to be possible only if the clouds are sufficiently high. The actual values are uncertain, but the facts we have considered indicate a height of the cloud tops in the range 400–600 hPa. Furthermore, CISK is possible in the convective boundary layer only if the precipitation is strong.

In the following, we shall attempt to combine all these points of view into a coherent picture of how heating by cumulus convection may contribute to the intensification of polar lows. The leading idea is that although this effect alone may not be able to produce a low, it can be responsible for the intense vortex often observed in the central part. The paper is organized in the following way. First we derive a CISK model which agrees with the idea that the convection takes place in a layer which is only marginally unstable (Section 2). The model gives sufficient growth rate to explain the formation of polar lows only if the convection is shallow (800–700 hPa). Besides, it does not give a clue to the problem of the scale of the disturbance. Since we have thrown doubt upon the effectivity of CISK for shallow convection and since there is evidence in favour of much higher cumulonimbus in the polar lows, we postulate the existence of localized deep instability (Section 3), and show how the horizontal scale may be determined by external influence (i.e., not chosen by the developing disturbance itself). In Section 4, it is shown that an increased growth rate is possible for a small-scale vortex imbedded in a low of somewhat larger dimension. A case study (Section 5) is intended to demonstrate some of the ideas in the paper.

2. A CISK model for the well-mixed layer

In theoretical studies of CISK, a crucial point is the height at which the heating by condensation takes place (i.e., the so-called "heating function"). Here, we propose another approach. In accordance with previous assumptions, we introduce as a constraint a fixed temperature lapse rate in the convective regime, while the mean temperature is allowed to change in space and with time. The lapse rate is chosen as dry adiabatic below 900 hPa (the condensation level) and moist adiabatic above. Strictly speaking, a change in the mean temperature leads to a change in the moist adiabatic lapse rate as well, in response to the dependency of the saturation vapour pressure on the temperature. However, we consider this change to be a second-order effect, so that one may choose a lapse rate corresponding to a specific adiabat, defined for instance by its wet-bulb potential temperature. As will be shown, this constraint makes possible a very simple linear CISK model where the heating profile is a consequence of the constraint.

There has been some doubt about the ability of the CISK concept to explain the development of a mature tropical cyclone from a small perturbation (Ooyama, 1982). Similar questions may be asked about its usefulness in connection with polar lows. A point of great interest has been the capacity of a CISK model to determine a preferred dimension of the growing disturbance. It has been shown by Emanuel (1983) and Bratseth (1985) that heating of an upper layer, and none below, leads to selection of a characteristic scale for maximum growth rate provided that the lower layer (i.e., the sub-cloud layer) is stably stratified in the sense that potential temperature increases upwards. The latter condition is especially apparent in Emanuel's derivation. However, in a convective boundary layer, the heating takes place at all heights and, furthermore, the static stability below the condensation level is slightly negative. Therefore, we are led to the conclusion that a free selection of a scale for maximum growth rate is in general not possible under such conditions. For this reason, we shall base our study on the hypothesis that the horizontal scale is determined by some other conditions, and we shall discuss possible mechanisms presently. A CISK model may still be useful since it provides an estimate of the intensification caused by the heating by condensation.

The linearized equations in isobaric coordinates take the form

$$\frac{\partial \zeta}{\partial t} = f\frac{\partial \omega}{\partial p}, \tag{1}$$

$$\frac{\partial T}{\partial t} = -\frac{T}{\theta}\frac{\partial \theta}{\partial p}\omega + \frac{q}{c_p}, \tag{2}$$

$$\frac{\partial \zeta}{\partial p} = -\frac{R}{fp}\nabla^2 T, \tag{3}$$

when standard notations are used. The geostrophic balance implied by (3) will be commented on later. The assumption that the vertical temperature profile is kept close to the adiabatic, is introduced into the above equations by means of

$$\frac{\partial T}{\partial t} = H(x, y, t). \tag{4}$$

Combining (1), (3) and (4) one gets

$$\frac{\partial^2 \omega}{\partial p^2} = -\frac{R}{f^2 p}\nabla^2 H, \tag{5}$$

which may be solved for ω with the boundary condition $\omega(p = p_0) = \omega_0$ and $\omega(p = p') = 0$. Here p_0 is taken to be 1000 hPa, and p' a pressure surface at the top of the convective layer. The solution is

$$\omega = \frac{-Rp_0}{f^2}\nabla^2 H\left(\xi \ln \xi - \frac{1-\xi}{1-\xi'}\xi' \ln \xi'\right) + \frac{\xi - \xi'}{1-\xi'}\omega_0, \tag{6}$$

where $\xi = p/p_0$ is the scaled pressure.

Next we relate q, the rate of diabatic heating per mass unit of air to Q, the total flux of heat into a column of air between the pressure surfaces p' and p_0. The relation is

$$Q = g^{-1}\int_{p'}^{p_0} q\,\mathrm{d}p, \tag{7}$$

where we may substitute for q from (2). Using (4) and (6), one gets after some straightforward arithmetic

$$\frac{c_p(p_0 - p')}{g}H - \frac{c_p(p_0 - p')}{g}L_*^2\nabla^2 H = \Lambda_0\omega_0 + Q, \tag{8}$$

where

$$L_*^2 = \frac{R}{f^2(1-\xi')}\int_{\xi'}^{1}\frac{\partial \theta}{\partial \xi} \times \xi^{\kappa}\left(\xi \ln \xi - \frac{1-\xi}{1-\xi'}\xi' \ln \xi'\right)\mathrm{d}\xi, \tag{9}$$

$$\Lambda_0 = -\frac{c_p}{g}\int_{\xi'}^{1}\frac{\partial \theta}{\partial \xi}\xi^{\kappa}\frac{\xi - \xi'}{1-\xi'}\mathrm{d}\xi, \tag{10}$$

and $\kappa = R/c_p$. If ω_0 and Q are known or parameterized, H may be determined from this equation. Then ζ can be derived by means of (6) and (1)

$$\frac{\partial \zeta}{\partial t} = -\frac{R}{f}\nabla^2 H\left(\ln \xi + 1 + \frac{\xi' \ln \xi'}{1-\xi'}\right) + \frac{f}{p_0 - p'}\omega_0. \tag{11}$$

We shall not search for exact solutions to the above equations, for instance in terms of specific normal mode solutions to (8). Instead, we note that the horizontal Laplacian of a field variable, for instance H, may be approximated by

$$\nabla^2 H = -L^{-2}H, \tag{12}$$

where L is a characteristic horizontal scale. Alternatively, we may consider (12) as a general form of a differential equation which, together with boundary conditions, gives normal mode solutions. Note that a double sine function with wavelength λ in both directions gives $L \simeq \lambda/9$. However, as shown by Bratseth (1985), this normal mode solution exaggerates the amplification rate since cooling of the same size as the heating is implicitly implied. In the formulation (12), such errors may be compensated for simply by choosing a somewhat larger value of L. Anyway, in view of the simplifications made in deriving the equations, and the fact that we shall be searching for only rough estimates of the intensification, the approximation (12) is considered to be acceptable.

Now H may be eliminated between (8), (11) and (12). The result is conveniently written as a prognostic equation for ζ_0, the 1000 hPa value of relative vorticity;

$$\frac{\partial \zeta_0}{\partial t} = A \frac{\Lambda_0 \omega_0 + Q}{L^2 + L_*^2} + \frac{f\omega_0}{p_0 - p'}. \tag{13}$$

Here

$$A = \frac{\kappa g}{f(p_0 - p')}\left(1 + \frac{\xi' \ln \xi'}{1 - \xi'}\right), \tag{14}$$

and L_* in fact, is Rossby's deformation radius.

In (13), ω_0 is the vertical velocity produced by the Ekman layer suction. The last term represents the spin-down effect produced by ω_0, while $\Lambda_0 \omega_0$ is tied to the adiabatic cooling brought about by a negative value of ω_0 (or vice versa).

To derive an Ekman layer CISK model, we express ω_0 in the usual way in terms of the surface geostrophic vorticity,

$$\omega_0 = -(\delta p)\zeta_0. \tag{15}$$

Furthermore, we assume that a certain fraction, K, of the water vapour convergence in the Ekman layer is condensed and the liberated latent heat given to an air column between the pressure surfaces p_0 and p'. The "efficiency factor" K is poorly known. Kuo (1965) assumes that a part of the vapour convergence is used to moisten the air column. We have previously pointed to the influence of precipitation on the release of latent heat in a convective boundary layer. We found that without precipitation, there may still be a net condensation related to the Ekman convergence, but that the influence on CISK is dubious. However, for simplicity we shall put $K = 1$ in all computations. Then

$$Q = -\Lambda \omega_0, \tag{16}$$

where $\Lambda = L_c r/g$. Here r is a representative mean mixing ratio of vapour in the boundary layer, and L_c is the latent heat of condensation.

As a numerical example, we have chosen the pseudoadiabatic temperature profile corresponding to a wet-bulb potential temperature of -2°C (Smithsonian Meteorological Tables, 1963). This temperature profile is used above 900 hPa, while a constant dry potential temperature of 273.5°K is used between 900 mb and 1000 mb. Furthermore, $\Lambda = 10^3$ m, corresponding to $r = 0.004$ while δp is 10 hPa. The last number corresponds to 100 m in metric units.

As foreseen, our result shows no maximum growth rate at non-zero values of L. In a slightly more complicated model, we have treated a surface layer (between 900 and 1000 hPa) separately, and joined it to the rest of the model by the appropriate internal boundary condition. As expected, this gave a reduced growth rate for the smallest scales, but only if the lowest layer had a non-zero static stability ($\partial\theta/\partial p \neq 0$) and no heat is added there. As mentioned earlier, neither of these remedies are in agreement with the basic assumptions for the present model. Heating below the condensation level may seem surprising at a first sight. However, it must be remembered that there is also a strong flux of sensible heat from the ocean.

Curves showing the exponential growth rate as a function of L are given in Fig. 1. The different curves correspond to different depths of the model, indicated on each curve by the scaled value of the top pressure surface. The corresponding values of L_*, also written on each curve,

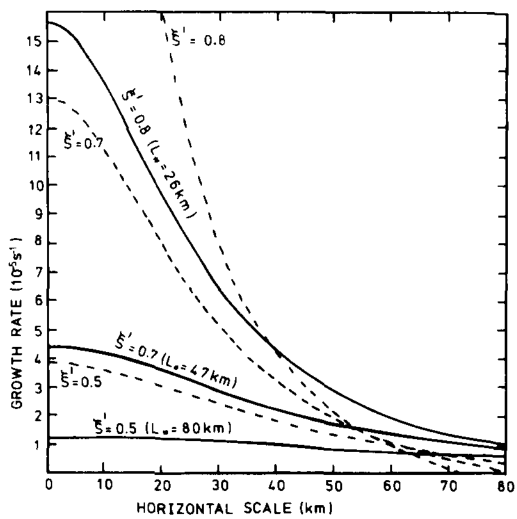

Fig. 1. Growth rate as a function of horizontal scale for 3 values of model depth (continuous lines). The corresponding values of the Rossby radius are written on each curve. Broken lines represent growth rate for a vortex imbedded in a larger low with relative vorticity equal to $2f$.

show an approximately linear variation with p'. The result is in fair agreement with other studies. A growth rate corresponding to the rapid intensification of a polar low is possible only for the shallow type (top surface at 800–700 hPa) and then only on a very short scale. (Note, however, that the characteristic horizontal scale, L, corresponds to only a fraction of the wavelength used in, for instance, Bratseth (1985).)

The conclusion of this section is that a CISK model operating in a well-mixed layer gives a significant growth rate only if it is shallow. However, for such layers, we have found that inefficient precipitation mechanisms may strongly reduce the rate of amplification. In addition, the fact that the model predicts a steady increase of the growth rate for decreasing horizontal scale, makes it impossible to isolate a *deterministic* mesoscale disturbance from the *probabilistic* convective scale with horizontal dimension of the same order of magnitude as the depth (Ooyama, 1982). For these reasons, we turn to another mechanism which we describe in Section 3.

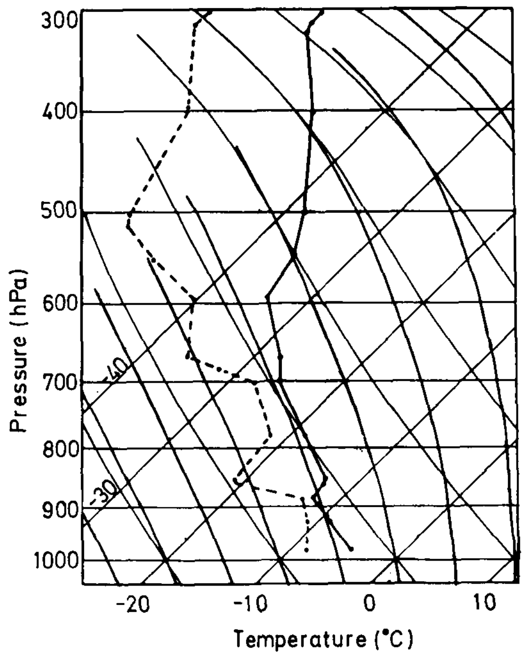

Fig. 2. Temperature (continuous line) and dewpoint (dashed line) at Bear Island on 00.00 GMT 2 November 1983, showing the convective boundary layer capped by an inversion at 880 mb, and a layer with small stability above.

3. Limited areas of deep convection

We have mentioned earlier that the convection may rise to greater heights when the static stability is low. In fact, although the winterly arctic air mass originally is very stable in its lower layers, the same is not necessarily the case at greater heights. This is exemplified in Fig. 2, where a boundary layer capped by an inversion underlies a layer of weak stability. Furthermore, such conditions may not be present over an extended region. For instance, restricted areas of less stable air may be connected to an upper air trough and advected with the air mass from the polar region (Rasmussen, 1985). Weak stability may also emerge in connection with baroclinic developments, as shown by Haugen (personal communication). In his numerical simulations of polar low developments, small-scale domains of weak stability are produced mainly as a consequence of vertical stretching. Note that in that case, cirrus clouds may be created by lifting of the air, in addition to the possible cumulonimbus activity.

As soon as the growing boundary layer has reached the base of the less stable air, the convection rapidly grows to much greater heights. When this happens in an area of restricted lateral extension, we shall refer to the phenomenon as a limited area of deep convection rather than the convective boundary layer, although the two are basically similar.

The lateral dimension of such a limited area of deep convection is determined by several parameters. Of essential importance is the degree of weak static stability, and the depth through which it occurs. If the base of an unstable layer has a minimum height somewhere, one may imagine that the deep convection starts in this location and expands laterally in response to the increase in the boundary layer thickness. A secondary circulation produced by convective heating may also influence the horizontal scale. However, it is obvious that the depth and degree of low static stability are of primary importance, and these parameters are determined basically by the synoptic scale conditions. We therefore conclude that under such circumstances, the horizontal scale of a secondary circulation, which may lead to vortex amplification, is determined mostly by external parameters and is *not* a result of a selection of the scale for maximum growth rate.

A limited area of deep convection obviously conforms to the constraint upon which we have built our CISK model. Since the scale is imposed by external conditions, we may use the model to estimate the growth rate of a small disturbance of given horizontal dimension. Since in this case the water precipitates much easier from the deeper clouds, the efficiency of CISK is presumably much greater than in the more shallow case. On the other hand, the greater depth gives smaller growth rate, according to Fig. 1. More rapid growth may nevertheless be obtained in the case of two interacting scales. This idea will be developed in Section 4.

4. Two interacting scales

Released from the steering wind field, a polar low most often has the shape of a vortex with approximately circular streamlines. Because of small dimension and strong winds, the absolute vorticity may be many times larger than the local value of the Coriolis parameter. Accordingly, the inertial stability becomes much larger than the characteristic synoptic scale value (Ooyama, 1982), and the deformation radius, proportional to the ratio between the static stability and inertial stability, becomes smaller. In general, a geostrophic balance, or rather the gradient wind relation, is a valid approximation for circulation systems with dimensions of the order of the deformation radius or larger. Thus, equation (3), or rather its gradient wind counterpart, may be valid even for very small scales.

We now assume that the circulation consists of two different scales, one which will be referred to as the mesoscale disturbance and another, somewhat larger one, which for short we will call the synoptic scale. The latter may for instance be the result of a baroclinic development on a shallow baroclinic zone (Haugen, personal communication). More specifically, we shall consider a small-scale vortex imbedded in a vortex of somewhat larger dimension. The latter will, for simplicity, be considered as barotropic and characterized by the relative vorticity $\bar{\zeta}$, independent of height and assumed to be uniform in the interior part where the mesoscale vortex is located. Furthermore, we consider the larger vortex, and especially $\bar{\zeta}$ to be independent of time, which means that the spin-down effect of the Ekman layer pumping is counteracted by some other energy source which we do not specify. Instead of (1), (2) and (3) we now get the perturbation equations

$$\frac{\partial \zeta}{\partial t} = (f + \bar{\zeta}) \frac{\partial \omega}{\partial p}, \tag{17}$$

$$\frac{\partial \zeta}{\partial p} = \frac{R}{fp} \nabla^2 T, \tag{18}$$

$$\frac{\partial T}{\partial t} = -\frac{\bar{T}}{\bar{\theta}} \frac{\partial \bar{\theta}}{\partial p} \omega + \frac{q}{c_p} = H, \tag{19}$$

where the variables ζ, ω and H refer to the mesoscale vortex. We then may derive equations similar to (12), (13), (14), (15) and (16) for the mesoscale vortex, with the difference that L_*^2 now contains $f(f + \bar{\zeta})$ instead of just f^2 (eq. (9)) and that the last term in (13) contains $(f + \bar{\zeta})$ instead of f.

In a tropical cyclone, the vorticity may be between one or two orders of magnitude larger than f. From polar low simulations, (Haugen, personal communication) we have computed values of $\bar{\zeta}$ more than 3 times f in disturbances which intensify because of baroclinic instability. As an example, we have chosen $\bar{\zeta} = 2f$, which brings L_*^2 down to one third of its previous value, and an increased rate of amplification which we have reproduced in Fig. 1 as broken lines. In the limit $L \to 0$, the amplification becomes 3 times stronger than in the previous case. For large values of L, the amplification is smaller than for $\bar{\zeta} = 0$, in response to the reduced value of L_*.

The amended amplification rates seem to be large enough to explain at least some cases of small-scale amplification. As an example, we shall briefly describe a characteristic case.

5. A case study

In the early morning of 25 April 1985, a mesoscale vortex moved along the coast of Western Norway from north to south. The maps

(Figs. 3 and 4) at the synoptic hours 00.00 GMT and 06.00 GMT show that the central pressure increased by about 5 hPa during this time period, possibly as a consequence of the fact that at this time, the low was partly located over land. Computed from the maps, the mean speed of displacement was about 15 m s^{-1}.

Fig. 5 shows the barograph record from an observing station on the coast. The location of the station is indicated by a thin arrow on Fig. 3. There is strong indication of a narrow inner core superimposed on a depression of larger dimension. The core passed by the observing station in about 2 h, corresponding to a diameter of 130 km, in reasonable agreement with the maps.

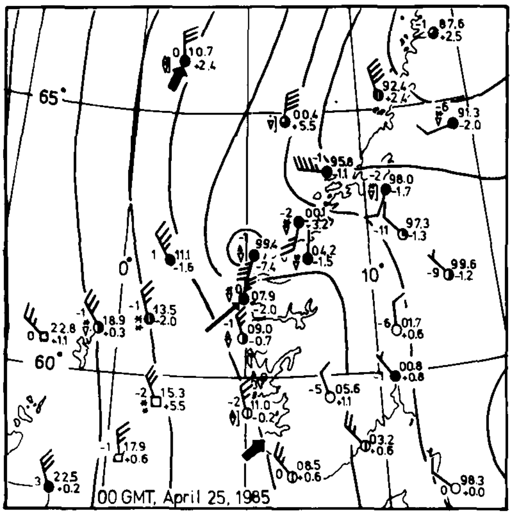

Fig. 3. Surface weather map for 00.00 GMT, 25 April 1985.

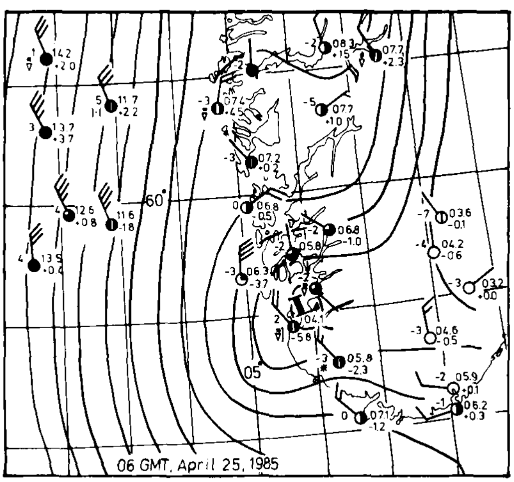

Fig. 4. Surface weather map for 06.00 GMT, 25 April 1985.

Figs. 6 and 7 show radiosonde ascents from two stations, indicated on Fig. 3 by thick arrows. Fig. 6, containing data from weather ship M (66°N, 2°E), shows the temperature and dewpoint on April 24 at 12.00 GMT (thin lines) and at 18.00 GMT (heavy lines). At 12.00 GMT, the top of the convective layer was located at 670 hPa. Above this layer, the atmosphere was very stable, with a gradual transition to stratospheric conditions which were found at above 470 hPa. Six hours later, the profile of temperature had changed significantly. The lower tropospheric layers were warmer and the upper ones were colder, indicating a reduced stability of the whole troposphere. Actually, the lapse rate conforms approximately to the moist adiabat, except in the layer between 550 and 700 hPa, which is slightly stable. Lack of observations prohibits an accurate surface analysis of this ocean area, but there are indications of a trough with a strong vorticity maximum having just passed by ship M at 18.00 GMT.

Judging from the sounding data described above, it is probable that an area with conditionally unstable stratification reaching above 500 hPa has been located in the vicinity of ship M at this time. This assumption is supported by the wind observations. Assuming geostrophic

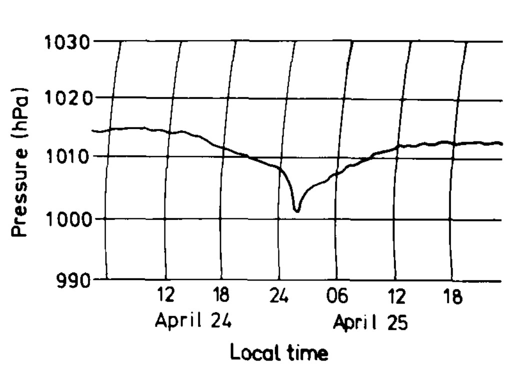

Fig. 5. Barograph record from the observing station Kinn (61.34°N, 4.46°E). The low centre passed over the station at about 01.00 GMT (02.00 local time).

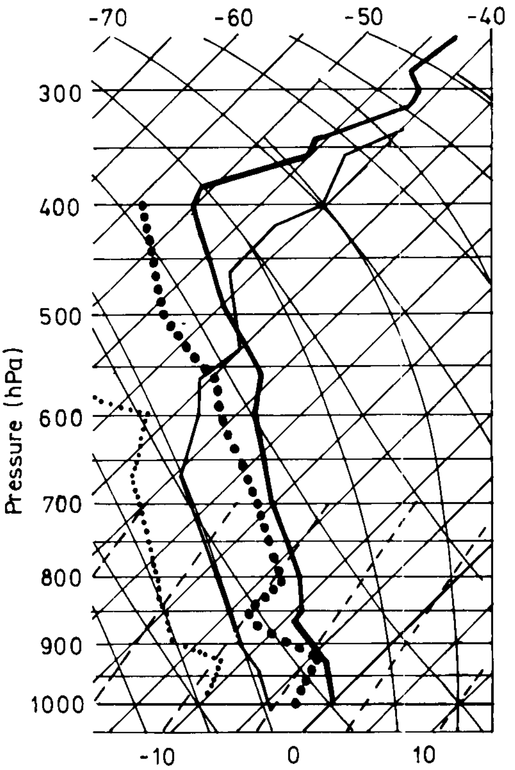

Fig. 6. Temperature soundings (continuous lines) and dewpoint (dotted lines) at weather ship M (66° N, 2° E). Heavy lines refer to 18.00 GMT, 24 April 1985, and thin lines to 12.00 GMT on the same date.

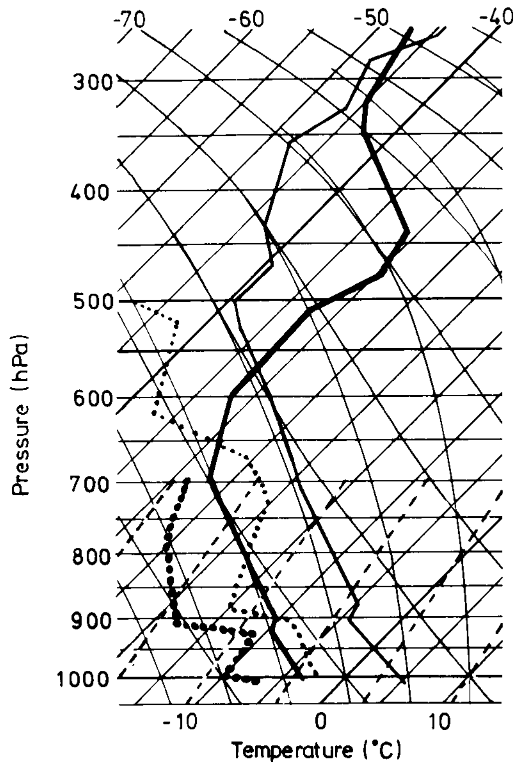

Fig. 7. Similar to Fig. 6, but at station Stavanger (58.58° N, 6.48° E). Heavy lines refer to 00.00 GMT, 25 April 1985, and thin lines to the ascent 12 hours later.

balance, the hodograph (not shown) indicates colder air to the west of the ship, especially between 600 and 500 hPa.

A similar change in the stability conditions connected with the passage of the low is demonstrated on Fig. 7, which shows radiosonde data from the station Stavanger (58.58° N, 6.48° E). Again, at 00.00 GMT on April 25, approximately 6 h before the low was closest to the station, there was a layer with generally weak stability below the 700 hPa level, and very stable air above (heavy lines). At 12.00 GMT (i.e., 6 h after the low passed by the station) the less stable layer had increased in thickness to 500 hPa. The thin layer of stable air at about 900 hPa, possibly caused by cooling over land during the night and early morning, was presumably prohibiting convection at the time of the soundings. However, because of the strong winds in the vicinity of the low, it is quite unlikely that this stable layer could have existed there, indicating that the convection probably reached the 500 hPa level.

How does the theoretical discussion above apply to the present case? As already noted, the vortex was in a state of decline during the 6 h we have followed it. The previous development can only be vaguely inferred from the scarce observations, notably from the weather ship. The general weather situation indicates that if the vortex was formed in the northern part of the Norwegian Sea, it must have grown to its observed strength in less than a day. A pressure trough of larger scale is indicated by the barograph record and also recognizable on the synoptic maps (not shown here). Estimates indicate $\bar{\zeta} = 2f$ in this trough at 700 mb (partly from strong horizontal wind shear). Nevertheless, there is little support for a rapid development to be found in the curves on Fig. 1 if $\zeta' = 0.5$ and L is taken to be equal to the observed radius of the core vortex. However, as indicated in Section 3, the appropriate value of L is much smaller. If we take the diameter previously determined (130 km) to be the dominating wavelength, a normal mode solution of the type used by Bratseth (1985) and others would indicate a value of L equal to 15 km, giving an e-folding time of about 7 h. This is not an impressive value, but it certainly indicates that the mechanisms we have described may contribute to the intensification of the mesoscale vortex.

6. Conclusion

This paper should not be looked upon as an attempt to explain the development of polar lows solely in terms of differential heating, and especially the heating by condensation. Rather, it is our belief that baroclinic and even barotropic instability are important and probably the dominating effects in many cases. The intention has been to show that heating by organized convection may in some cases be of importance, and especially may have a modifying influence on already existing lows. Our analysis shows that the effect may be significant only for very small-scale vortices, which form in an environment of considerable cyclone vorticity and generally weak static stability (see also Rabbe, 1987).

Fig. 8 shows a schematic cross section through a polar low, indicating the structure we have proposed in the previous sections. The general (northerly) wind direction is from right to left, and the height of the boundary layer top (GG′) increases downwind. In the section SS′, there is particularly low stability in the upper layers and accordingly a limited area of deep convection which rises to much greater heights. Secondary circulation is indicated by heavy continuous stream lines, and Ekman layer inflow by arrows. Cirrus shield is shown to extend downwind from the cumulonimbus tops. The whole cross section may be contained in a circulation of larger dimension, giving increased rotational stability and growth rate.

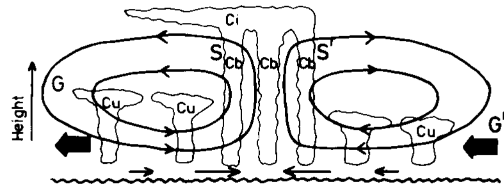

Fig. 8. Schematic cross section illustrating some of the principal ideas outlined in the paper. See text for further explanation.

The above ideas are rather speculative since the observational support is far from conclusive. Crucial points are the depth of the boundary layer, the height of the cirrus clouds and their connection to the convection in the boundary layer. It is surprising that these questions have hitherto attracted so little attention.

7. Acknowledgements

The author is indebted to Professor Hilding Sundqvist for constructive comments on the manuscript. This work has been supported financially by The Norwegian Meteorological Institute as a part of The Polar Lows Project. Maps, barograph records and radiosondes have been provided by Mr. M. Naustvik and Mr. S. Hoppestad.

REFERENCES

Bratseth, A. M. 1985. A note on CISK in polar air masses. *Tellus 37A*, Polar Low Special Issue, 403–406.

Businger, S. 1985. The synoptic climatology of polar low outbreaks. *Tellus 37A*, Polar Low Special Issue, 419–432.

Eliassen, A. and Kleinschmidt, E. 1957. Dynamic meteorology. *Handb. Phys., Berlin 48*, 19.

Emanuel, K. A. 1983. Elementary aspects of the interaction between cumulus convection and the large-scale environment. *Mesoscale meteorology—theory, observations and models*, (eds.: D. K. Lilly and T. Gal-Chen). Dordrecht-Boston, D. Reidel Publishing Co., 551–575.

Ese, T., Kanestrøm, I. and Pedersen, K. 1985. Polar lows in the Norwegian Sea and the Barents Sea. A climatological study. *Technical Report No. 16, The polar lows project*. The Norwegian Meteorological Institute, Oslo, Norway.

Grønås, S., Foss, A. and Lystad, M. 1987. Numerical simulations of polar lows in the Norwegian Sea. *Tellus 39A*, 334–353.

Holton, J. R. 1979. *An introduction to dynamic meteorology*. Academic Press.

Kuo, H. L. 1965. On formation and intensification of tropical cyclones through latent heat release by cumulus convection. *J. Atmos. Sci. 22*, 40–63.

Kuo, H. L. 1973. Nonlinear theory of the formation and structure of the intertropical convergence zone. *J. Atmos. Sci. 30*, 969–983.

Lilly, D. K. 1968. Models of cloud-topped mixed layers under a strong inversion. *Q.J.R. Meteorol. Soc. 94*, 292–309.

Ooyama, K. 1969. Numerical simulations of the life cycle of tropical cyclones. *J. Atmos. Sci. 26*, 3–40.

Ooyama, K. V. 1982. Conceptual evolution of the theory and modelling of the tropical cyclone. *J. Meteorol. Soc. Japan 60*, 369–379.

Økland, H. 1983. Modelling the height, temperature and relative humidity of a well-mixed planetary boundary layer over a water surface. *Boundary-Layer Meteorol. 25*, 121–141.

Rabbe, Å. 1975. Arctic instability lows. *Meteorologiske Annaler*, No. *6*. The Norwegian Meteorological Institute, Oslo, Norway, 303–329.

Rabbe, Å. 1987. A polar low over the Norwegian Sea, 29 February–1 March 1984. *Tellus 39A*, 326–333.

Rasmussen, E. 1979. The polar low as an extra tropical CISK disturbance. *Q.J.R. Meteorol. Soc. 105*, 531–549.

Rasmussen, E. 1985. A case study of a polar low development over the Barents Sea. *Tellus 37A*, Polar Low Special Issue, 407–418.

Schubert, W. H., Wakefield, J. S., Steiner, E. J. and Cox, S. K. 1979. Marine stratocumulus convection. Part II: Horizontally inhomogeneous solutions. *J. Atmos. Sci. 36*, 1308–1324.

Smithsonian Meteorological Tables, 1963. *The Smithsonian Institute*, Washington D.C.

Wallace, J. M. and Hobbs, P. V. 1977. *Atmospheric science. An introductory survey*, ch. 4. Academic Press.